

Detection of tumors on brain MRI images using the hybrid convolutional neural network architecture

Ahmet Çınar, Muhammed Yildirim*

Computer Engineering Department, Firat University, Elazığ, Turkey

ARTICLE INFO

Keywords:

Brain Tumor
Classification
CNN
Deep Learning
Machine Learning

ABSTRACT

Brain tumor is one of the dangerous and deadly cancer types seen in adults and children. Early and accurate diagnosis of brain tumor is important for the treatment process. It is an important step for specialists to detect the brain tumor using computer aided systems. These systems allow specialists to perform tumor detection more easily. However, mistakes made with traditional methods are also prevented. In this paper, it is aimed to diagnose the brain tumor using MRI images. CNN models, one of the deep learning networks, are used for the diagnosis process. Resnet50 architecture, one of the CNN models, is used as the base. The last 5 layers of the Resnet50 model have been removed and added 8 new layers. With this model, 97.2% accuracy value is obtained. Also, results are obtained with Alexnet, Resnet50, Densenet201, InceptionV3 and Googlenet models. Of all these models, the model developed with the highest performance has classified the brain tumor images. As a result, when analyzed in other studies in the literature, it is concluded that the developed method is effective and can be used in computer-aided systems to detect brain tumor.

Introduction

The brain is one of the most complex mechanisms in the human body, made up of billions of cells. A brain tumor can be expressed as a tissue that occurs in a place where it should not be in our brain or an uncontrolled growth of any tissue where it should not be. Early and correct detection of brain tumor has a very important place in this type of cancer, which is fatal [1]. In this study, the classification process was carried out using MRI images. Networks must be trained with large databases before this process can be done. In this paper, deep learning methods are used which can produce successful results in large databases. Thanks to computer-aided systems, experts can diagnose the disease. In this way, mistakes that may arise in traditional methods are prevented [2]. There are studies in the literature using different models and architectures [3].

Afshar et al. introduced a method they developed to classify brain tumor images. In the method they recommended, they used 1 convolutional layer with 64 feature maps and 16 primary capsules. They achieved an accuracy rate of 86.56%. In the same study, they compared the model they developed with CNN and obtained an accuracy value of 72.13 [4].

Saxena et al. used Vgg16, InceptionV3 and Resnet50 models to classify brain tumor data in their study. In this study they conducted

with transfer learning methods, they obtained the highest accuracy rate in the Resnet50 model with 95% [5].

Shahzadi et al. used the Cnn - Lstm hybrid construct to classify brain tumor cells. They stated that they classified the network with 71% accuracy with Alexnet-Lstm, with 84% accuracy with VggNet-Lstm and with 71% accuracy with Resnet-Lstm. They achieved the highest accuracy rate in VggNet-Lstm architecture with 84% [6].

El Abbadi et al. used Singular Value Decomposition (SVD) in their study to classify brain tumor data. They tested their methods using 20 normal and 50 abnormal data. They stated that they obtained 96.66% accuracy rate, 90% Sensitivity and 98% Specificity value [7].

Mohsen et al. proposed a new model to classify brain tumor data using Discrete Wavelet Transform (DWT) using deep learning methods. With this model they proposed, they achieved an accuracy of 93.94%. They compared this model proposed in the same study with the Deep Learning and KNN models [8].

Charfi et al. introduced a method developed for the classification of brain tumor MR images. He stated that he used histogram equalization method for image segmentation in his proposed machine learning method. He then used PCA to reduce the size of the data obtained. And finally used feed forward back propagation neural network for classification process. He obtained 90% accuracy in the images he classified as normal and abnormal. He stated that this accuracy rate is very good

* Corresponding author.

E-mail addresses: acinar@firat.edu.tr (A. Çınar), 171129205@firat.edu.tr (M. Yildirim).

<https://doi.org/10.1016/j.mehy.2020.109684>

Received 5 February 2020; Received in revised form 6 March 2020; Accepted 18 March 2020

0306-9877/ © 2020 Elsevier Ltd. All rights reserved.

[9].

Vani et al. Stated that they used SVM to classify brain tumor data. In their study, they stated that they correctly predicted 82% positive data and 81.48% correctly predicted Negative data [10].

Gupta et al. Performed the classification using Brain Tumor MRI images in their study. They used Discrete Wavelet transform (DWT), PCA and SVM for classification. They obtained 80% accuracy rate, 84% sensitivity and 92% specificity rate. They stated that their study could be used in a clinical setting [11].

Citak et al. Stated that they used 3 different machine learning algorithms in their study on brain tumor. They stated that these algorithms are SVM, multi-layer perceptrons and logistic regression. As a result, they achieved 93% accuracy, 86.7% specificity, and 96.4% sensitivity [12].

In the second part of the article, the Material and Methods section is discussed. In this section, the data set used, Deep learning, Cnn and Cnn Layers are examined. Then, the improved model was introduced. In the third section, there is the Application and Results section. In the last section, the conclusion obtained and the studies planned for the future are mentioned.

Material and methods

In this paper, deep learning methods, a sub-branch of machine learning, are used. Deep learning methods can produce successful results in large databases. The data set is classified primarily with the CNN models, Alexnet [13], Resnet50 [14], Densenet201 [15], Googlenet [16] and InceptionV3 [17] models. In addition, the data set is trained with the model improved. The results obtained are interpreted in detail in the Application and Results section with tables and graphics.

In this section, Deep learning, CNN, Dataset, Structure of the improved model, CNN layers used in the improved model are examined.

Dataset

The brain tumor MRI images used in this study were taken from the Brain MRI Images for Brain Tumor Detection dataset from the Kaggle site [18]. The dataset consists of 2 folders. In the first folder there are 98 pictures without tumor, while in the second folder there are 155 tumor pictures. Picture example in the dataset is as in Fig. 1.

Deep learning

Deep learning models have increased their popularity by winning more than one competition recently. Particularly, in 2012, Alexnet

model winning the Imagenet competition was an important turning point. The biggest difference that distinguishes deep learning networks from artificial neural networks is that deep learning networks consist of multiple layers [19]. The output value of each layer is designed to be the input value of the next layer. Deep learning networks work with large databases. Also, since these networks consist of more than one layer, the cards used must be strong [20]. Recently, strong GPU cards are produced. There is no need to pre-process data from deep learning networks. Deep learning networks can work directly with raw data.

CNN architectures are frequently used in object recognition applications. CNN architectures are usually created using the input layer, the convolution layer, the pooling layer, the fully connected layer, and the output layers. Different models are created with different layouts of these layers.

Structure of system

In improved method, the winner of the 2015 ILSVRC ImageNet competition, the Resnet50 model is used as the base. Instead of building a new network, it is preferred to use a trained model. The reason for using Resnet50 model's as base is that it is desirable to benefit from the accumulation of this previously trained network, and that Resnet50 model's has achieved successful results in biomedical data.

In the developed model, the last 5 layers of Resnet50 have been removed. 10 new layers have been added instead of these 5 layers. The number of layers from 177 increased to 182. The structure of the developed model is given in Fig. 2.

Layer order is important in hybrid structures and developments to be made in CNN architecture used in deep learning. In our study, the last five layers of Resnet50 architecture have been removed and 10 new layers have been added instead, without disturbing the CNN architecture. This addition order is based on CNN theory knowledge. These layers are Relu, BatchNormalization, Dropout, Fullyconnected, Relu, Maxpooling, FullyConnected, Softmax and Classification layers, respectively.

The names, parameter numbers and other features of the added layers are as in Table 1.

Input layer

It is the first layer of the designed architecture of the input layer. The data is read from this layer. Reading size of the models used in the application is given in Table 2.

Convolutional layer

The convolution process is a customized linear process. Here, instead of matrix multiplication, convolution is performed. The purpose of this layer can be briefly defined as producing feature maps [21]. Eq. (1) is used for the discrete time convolution process.

$$s(t) = (x * w)(t) = \sum_{a=-\infty}^{\infty} x(a)w(t-a) \quad (1)$$

w : kernel (filter), x : input, t : times, s : Result

If two-dimensional data such as pictures are to be used as input, Eq. (2) is used.

$$S(i, j) = (I * K)(i, j) = \sum_m \sum_n I(i, j)K(i-m, j-n) \quad (2)$$

The terms i and j refer to the positions of the new matrix to be obtained as a result of the convolution process. It is usually positioned so that the center of the filter is at the origin.

If Cross Entropy is to be applied, Eq. (3) should be used.

$$S(i, j) = (I * K)(i, j) = \sum_m \sum_n (i+m, j+n)K(m, n) \quad (3)$$

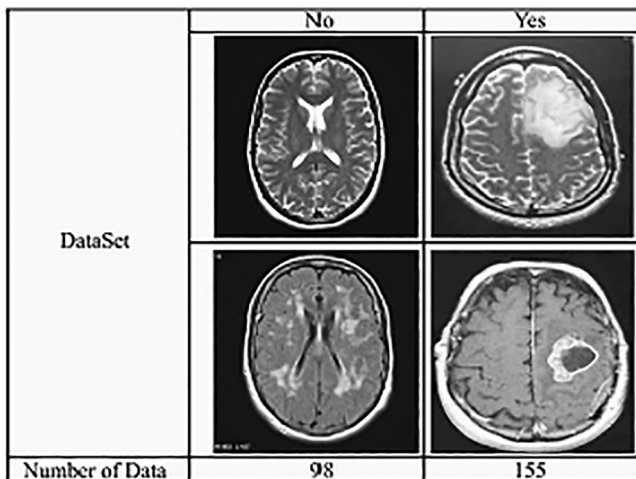


Fig. 1. Image examples used in the paper.

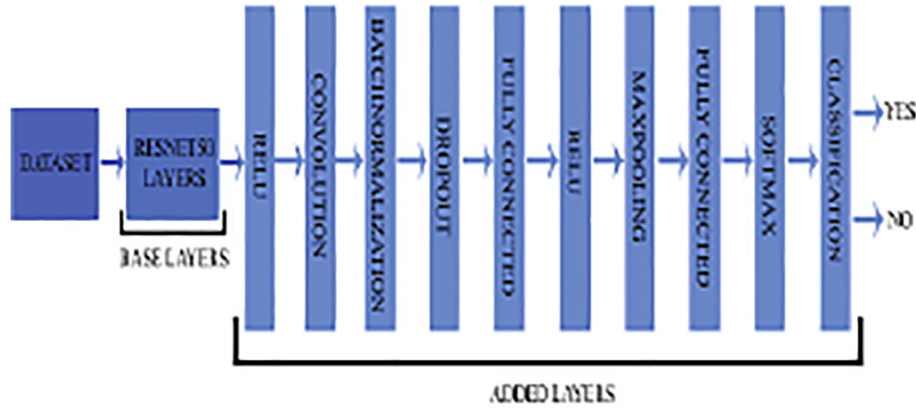


Fig. 2. Structure of the Improved Model.

Table 1
Properties of Added Layers.

Analysis Result			
	Name	Type	Activations
1	Imageinput	Image Input	$224 \times 224 \times 1$
2	conv_1	Convolution	$112 \times 112 \times 64$
172	add_16	Addition	$7 \times 7 \times 2048$
173	Relu	Relu	$7 \times 7 \times 2048$
174	conv_2	Convolution	$7 \times 7 \times 32$
175	Batchnorm	Batch Normalization	$7 \times 7 \times 32$
176	Dropout	Dropout	$7 \times 7 \times 32$
177	fc_1	Fully Connected	$1 \times 1 \times 2$
178	activation	Relu	$1 \times 1 \times 2$
179	Maxpool	Max Pooling	$1 \times 1 \times 2$
180	fc_2	Fully Connected	$1 \times 1 \times 2$
181	fc1000_soft	Softmax	$1 \times 1 \times 2$
182	Classoutput	Classification Output	–

Table 2
Input Size of Image.

Model	Input Size of Image
Alexnet	227 227 1
Resnet50	224 224 1
Densenet201	224 224 1
Inceptionv3	299 299 1
Googlenet	224 224 1
Improved Model	224 224 1

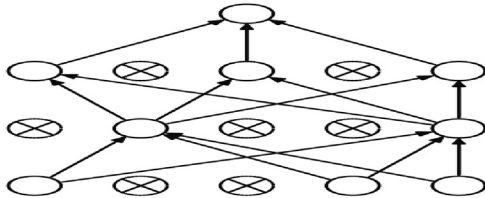


Fig. 3. Node Reduction with the Dropout Process.

Activation function

The conversion of the value obtained in deep learning studies to non-linear is realized by using activation functions. Activation functions are used for non-linear transformation processes in multi-layer artificial neural networks. There are multiple activation functions [22]. Tanh, Sigmoid and Relu are the most commonly used. Relu was used in the developed method.

$$\text{Sigmoid: } f(x) = \frac{1}{1 + e^{-x}}, f'(x) = f(x)(1 - f(x)) \quad (4)$$

Table 3
Confusion Matrix.

	Normal	Tumor
Normal	TP	FN
Tumor	FP	TN

True-Positive (TP): The brain tumor image is predicted to be normal and this image is really normal.

True-Negative (TN): The brain tumor image is predicted to be tumor and this image is really tumor.

False-Positive (FP): The brain tumor image is predicted to be tumor but this image is normal.

False-Negative (FN): The brain tumor image is predicted to be normal but this image is tumor.

Accuracy: Accuracy value is the ratio of the number of correctly predicted images to the total number of images used in the test operation[29]. How the accuracy value is calculated is given in equation (17).

Table 4
Main values used when training networks.

Solver Name	Sgdm
MiniBatchSize	16
MaxEpochs	5
InitialLearnRate	1.0000e-04
Shuffle	every-epoch
ValidationFrequency	3
Total Iteration	160

$$\text{Tanh: } f(x) = \tanh(x) = \frac{2}{1 + e^{-2x}} - 1, f'(x) = 1 - f(x)^2 \quad (5)$$

$$\text{Relu: } f(x) = \begin{cases} 0, & x < 0 \\ x, & x \geq 0 \end{cases}, f'(x) = \begin{cases} 0, & x < 0 \\ 1, & x \geq 0 \end{cases} \quad (6)$$

Normalization

Used to normalize the output of convolution or fully connected layers. This process, which usually takes place before the activation function, normalizes the layer output. Thanks to this process, the training of the network takes place more quickly. In addition, the covariance shift is reduced by the batch normalization process [23]. The declaration that performs the batch-normalization process is 7.

$$Y_i = \frac{X_i - \mu_\beta}{\sqrt{\sigma_\beta^2 + \epsilon}} \quad (7)$$

$$\sigma_\beta = \frac{1}{M} \sum_{i=1}^M (X_i - \mu_\beta)^2 \quad (8)$$

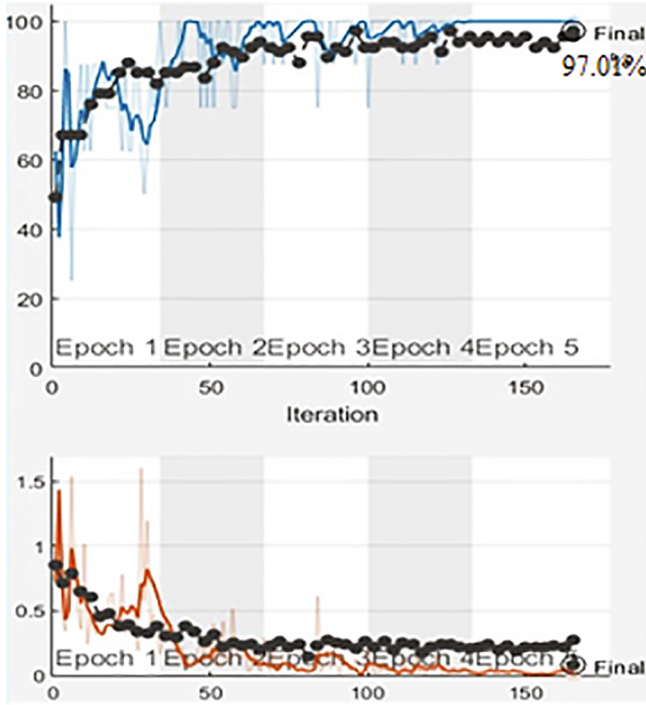


Fig. 4. Training Curves of the Improved Model.

Table 5

Performance criteria of the Improved model.

Confusion Matris	36	–
	2	29
Accuracy	97.01	
Sensitivity	94.7	
Specificity	100	
F-Measure	96.90	
FPR	0	
FDR	0	
FNR	0.0526	

$$\mu_{\beta} = \frac{1}{M} \sum_{i=1}^M X_i \quad (9)$$

M: Number of input data

 X_i : $i = 1 \dots M$ μ_{β} : Average value of the stack, σ_{β} : Standard deviation of the stack, Y_i : New values resulting from normalization process

Dropout

A model can memorize training data and lose its ability to generalize. The dropout layer provides prevention of over-learning by randomly dropping nodes and connections during the training of the network. Thanks to this process, weights are prevented from over-matching the data. Dropout layer can only be used to prevent over-learning during training [24]. Dropout is not used for testing and verification. A typical dropout operation is as in Fig. 3.

Fully connected

Neurons in the fully connected layer depend on all areas of the previous layer. Data from the previous layer is converted into a one-dimensional matrix in this layer. The number of fully onnected layers used in each model may differ[25]. In this layer, equation (10) is used for feed forward.

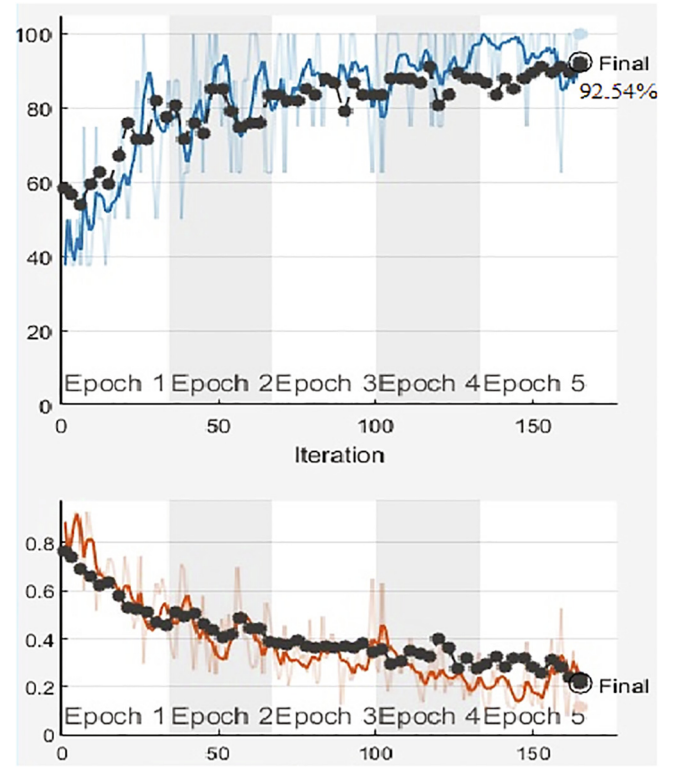


Fig. 5. Training curves of the Resnet50.

Table 6

Performance criteria of the Resnet50.

Confusion Matris	35	1
	4	27
Accuracy	92.54	
Sensitivity	89.74	
Specificity	96.4	
F-Measure	93.33	
FPR	0.0357	
FDR	0.0278	
FNR	0.1026	

$$u_i^l = \sum_j w_{ji}^{l-1} y_j^{l-1} \quad (10)$$

$$y_i^l = f(u_i^l) + b^{(l)} \quad (11)$$

l : Layer number, i, j : Neuron number, y_i^l : the value in the output layer created, w_{ji}^{l-1} : The weight value in the hidden layer, y_j^{l-1} : The value of input neurons, u_i^l : The value of the output layer before the activation function, $b^{(l)}$: deviation value.

The output value of the fully connected layer used in the developed model is set to 2 because we have 2 classes.

Pooling layer

The pooling layer is usually used after the convolutional layer. The task of the pooling layer is to simplify the information in the output of the convolutional layer. The pooling layer takes each feature map information from the convolutional layer and prepares a condensed feature map. Avaragepooling and max-pooling are the most common methods [26]. No learning process takes place in this layer. NxN size filters are selected in this layer. The size of the image resulting from the pooling layer is given in Eq. (12).

$$S = w2 * h2 * d2 \quad (12)$$

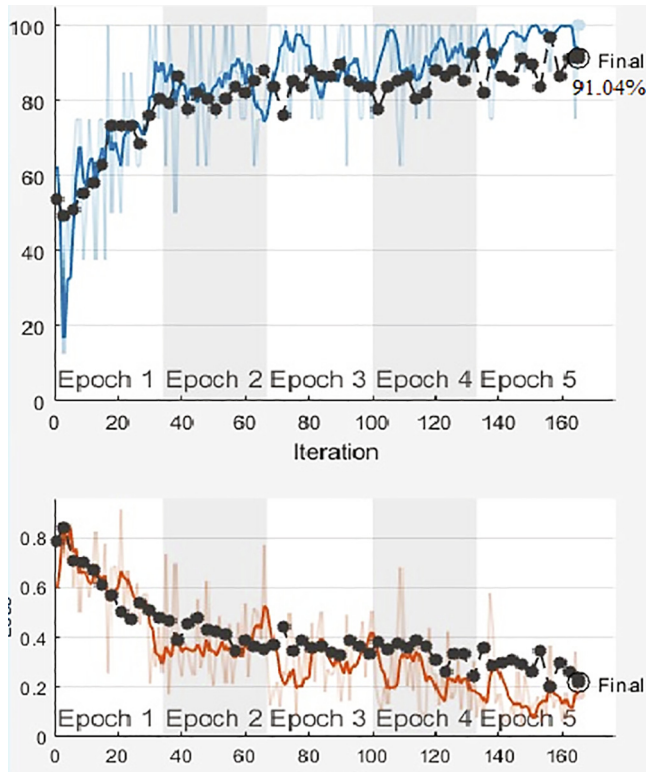


Fig. 6. Training curves of the Densenet201.

Table 7
Performance criteria of the Densenet201.

Confusion Matrix	36	–
	6	25
Accuracy	91.04	
Sensitivity	85.71	
Specificity	100	
F-Measure	92.30	
FPR	0	
FDR	0	
FNR	0.1429	

$$w2 = \frac{(w1 - f)}{A + 1} \quad (13)$$

$$h2 = \frac{h1 - f}{A + 1} \quad (14)$$

$$d2 = d1 \quad (15)$$

$w1$ = width of the input image, $h1$ = height of the input image, $d1$ = depth value of input image size, f = filter size, A = number of steps used, S = Size of manufactured image.

Max-pooling was used in the improved model.

Softmax

Softmax is used before the Classification layer. It generates a value for each class by performing the probabilistic calculation created on the network [27]. This layer performs the calculated probabilities for each class with equation (16).

$$P(y = j|x; W, b) = \frac{\exp^{x^T w_j}}{\sum_{j=1}^n \exp^{x^T w_j}} \quad (16)$$

W, b, sa : weight vector.

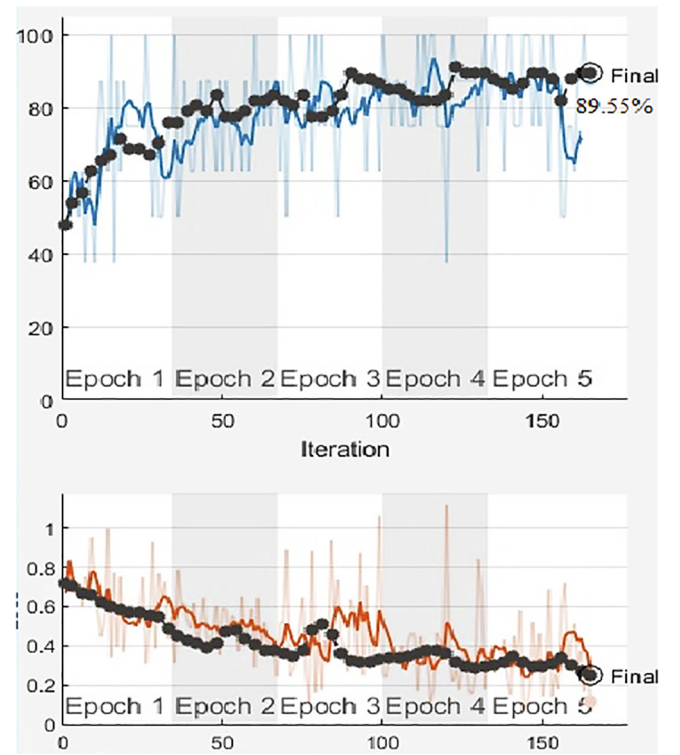


Fig. 7. Training curves of the Alexnet.

Table 8
Performance criteria of the Alexnet.

Confusion Matrix	34	2
	5	26
Accuracy	89.55	
Sensitivity	87.17	
Specificity	92.85	
F-Measure	90.05	
FPR	0.0714	
FDR	0.0556	
FNR	0.1282	

Classification layer

This layer used after the Softmax layer is the last layer of the network. The output value of this layer is equal to the number of classes produced. In this study, it is tumor and normal.

Application and results

In this paper, it is aimed to classify brain tumor MRI images. The network is primarily trained with the MRI images in the dataset. The system is then tested with normal and tumor images. The application was obtained in Matlab environment [28] with a computer with i7 processor, GPU card and 8 GB Ram.

One of the most important values used in the classification process in deep learning networks is the Confusion matrix. Other used values are obtained from the Confusion matrix. In short, the confusion matrix is the summary of the trained network, it shows the performance of the network. A general Confusion matrix is shown in Table 3.

$$Accuracy = \frac{TP + TN}{TP + TN + FP + FN} \quad (17)$$

Sensitivity: It is achieved by dividing the size of correctly estimated data by the whole size of correct data. Eq. (18) is used to obtain the sensitivity value.

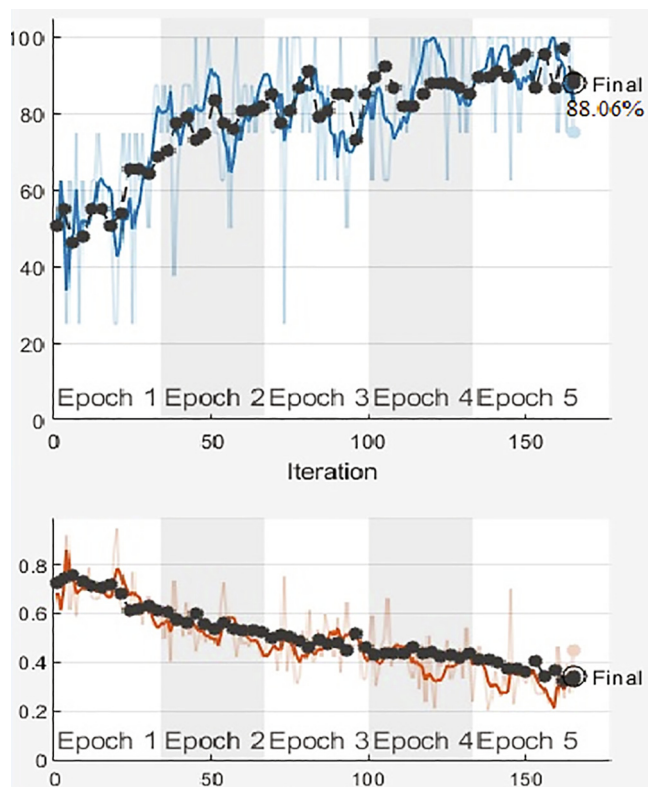


Fig. 8. Training curves of the InceptionV3.

Table 9
Performance criteria of the Inceptionv3.

Confusion Matrix	36	–
	8	23
Accuracy	88.06	
Sensitivity	81.81	
Specificity	100	
F-Measure	89.99	
FPR	0	
FDR	0	
FNR	0.1818	

$$\text{Sensitivity} = \frac{TP}{TP + FN} \quad (18)$$

Specificity: It is obtained by dividing the correctly estimated negative values by the total number of negative values. Eq. (19) is used to obtain the Specificity value.

$$\text{Specificity} = \frac{TN}{TN + FP} \quad (19)$$

F-measure: F-measure value is obtained using the Precision and Recall values [30]. Eq. (20) is used to obtain the F-measure value.

$$F - \text{measure} = \frac{2 * \text{Precision} * \text{Recall}}{\text{Precision} + \text{Recall}} \quad (20)$$

$$\text{Precision} = \frac{TP}{TP + FP} \quad (21)$$

$$\text{Recall} = \frac{TP}{TP + FN} \quad (22)$$

$$\text{FalsePositiveRate: FPR} = \frac{FP}{FP + TN} \quad (23)$$

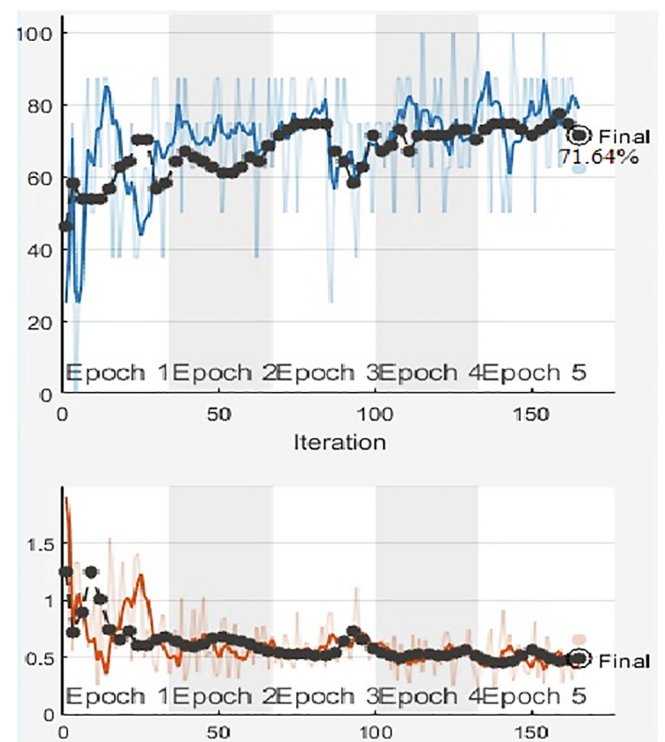


Fig. 9. Training curves of the Googlenet.

Table 10
Performance criteria of the Googlenet.

Confusion Matrix	35	1
	18	13
Accuracy	71.64	
Sensitivity	66.03	
Specificity	92.85	
F-Measure	66.03	
FPR	0.0714	
FDR	0.0278	
FNR	0.3396	

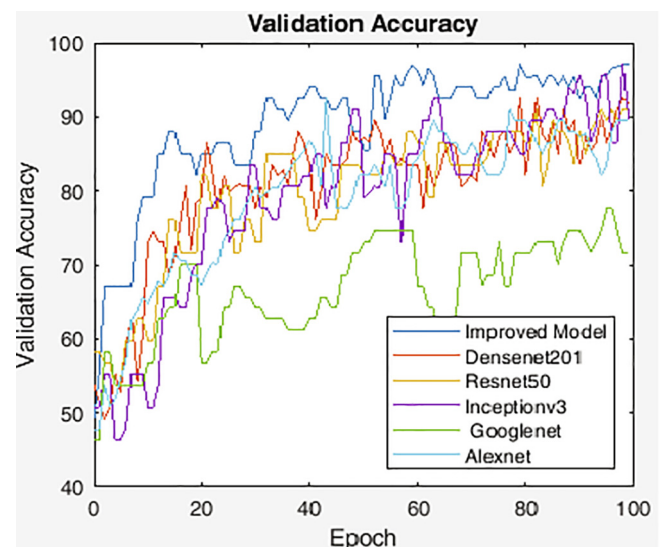


Fig. 10. Accuracy curves of the models used when training networks.

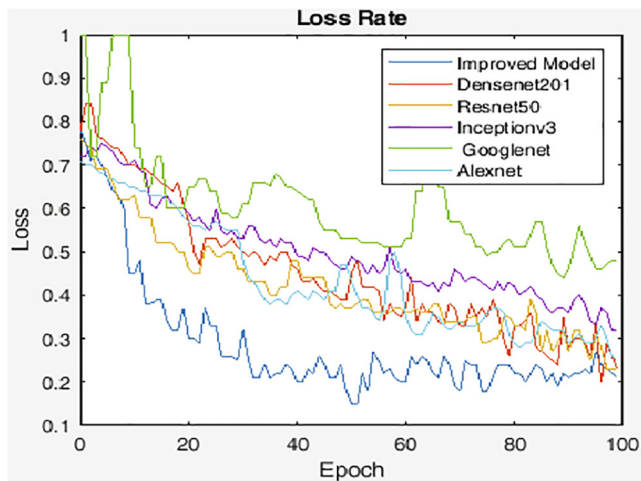


Fig. 11. Loss curves of models used when training networks.

Table 11
Performance Criteria of All Models.

	Accuracy	FPR	FDR	FNR
Improved Model	97.01	0	0	0.0526
Densenet201	91.04	0	0	0.1429
Resnet50	92.54	0.0357	0.0278	0.1026
Inceptionv3	88.06	0	0	0.1818
Googlenet	71.64	0.0714	0.0278	0.3396
Alexnet	89.55	0.0714	0.0556	0.1282

Table 12
Accuracy and Values of Models.

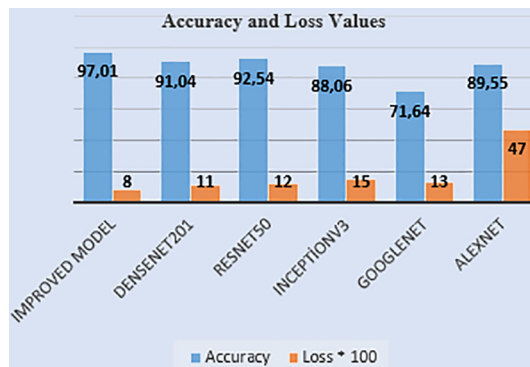


Table 13
Studies on brain tumor.

Authors/Year	Methods	Accuracy
Afshar et al.[4] /2018	Improved Method	86.56%
Saxena et al.[5] /2019	Resnet50	95%
Shahzadi et al.[6] /2018	VggNet – Lstm	84%
El Abbadi et al.[7] /2016	SVD	96.66%
Mohsen et al.[8] /2018	DWT	93.94%
Charfi et al[9] /2014	PCA	90%
Vani et al.[10] /2017	SVM	81.48%
Gupta et al.[11] /2017	DWT, PCA, SVM	80%
Citak et al. [12] /2018	SVM, multi-layer perceptrons and logistic regression	93%
Proposed Method /2020	Improved Model	97.01

$$\text{FalseDiscoveryRate: } FDR = \frac{FP}{FP + TP} \quad (24)$$

$$\text{FalseNegativeRate: } FDR = \frac{FN}{FN + TP} \quad (25)$$

The values given in Table 4 were used while training the networks with CNN models and the developed model.

The accuracy and loss curve obtained while training the network with the developed model is given in Fig. 4. As seen in Figure 4, 97.2% accuracy rate was obtained while training the network with the developed model.

After the network was trained with the developed model, as seen in Table 5, F-measure value of 96.90%, Specificity value of 100%, Sensitivity value of 94.7%, FPR value 0, FDR value 0, FNR value 0.0526 and accuracy value of 97.01% were obtained.

As seen in the Confusion matrix given in Table 5, the improved model correctly classified 36 of 36 normal images. In addition, he predicted 29 of 31 brain tumor images correctly, and 2 predicted brain tumor images incorrectly.

The accuracy and loss curve obtained while training the network with the Resnet50 model is given in Fig. 5. As seen in Figure 5, 92.54% accuracy rate was obtained while training the network with Resnet50 model.

After training the network with Resnet50 model, as seen in Table 6, F-measure value of 93.33%, Specificity value of 96.4%, Sensitivity value of 89.74%, FPR value 0.0357, FDR value 0.0278, FNR value 0.1026 and accuracy value of 92.54% were obtained.

As seen in the Confusion matrix given in Table 6, the Resnet50 model correctly classified 35 of 36 normal images. However, he estimated 1 normal images as brain tumors. In addition, while predicting 27 of 31 brain tumor images correctly, and predicted 4 brain tumor images incorrectly.

The accuracy and loss curve obtained while training the network with Densenet 201 model is given in Fig. 6. As seen in Figure 6, 91.04% accuracy rate was obtained while training the network with the Densenet201 model.

After training the network with Densenet201 model, as seen in Table 7, F-measure value of 92.30%, Specificity value of 100%, Sensitivity value of 85.71%, FPR value 0, FDR value 0, FNR value 0.1429 and accuracy value of 91.04% were obtained.

As seen in the Confusion matrix given in Table 7, the Densenet201 correctly classified 36 of 36 normal images. In addition, he predicted 25 of 31 brain tumor images correctly, and 6 predicted brain tumor images incorrectly.

The accuracy and loss curve obtained while training the network with the Alexnet model is given in Fig. 7. As seen in Figure 7, 89.55% accuracy rate was obtained while training the network with Alexnet model.

After training the network with Alexnet model, as seen in Table 8, F-measure value of 90.05%, Specificity value of 92.85%, Sensitivity value of 87.17%, FPR value 0.0714, FDR value 0.0556, FNR value 0.1282 and accuracy value of 89.55% were obtained.

As seen in the Confusion matrix given in Table 8, the Alexnet correctly classified 34 of 36 normal images. However, he estimated 2 normal images as brain tumors. In addition, he predicted 26 of 31 brain tumor images correctly, and 5 predicted brain tumor images incorrectly.

The accuracy and loss curve obtained while training the network with the Inceptionv3 model is given in Fig. 8. As seen in Figure 8, 88.06% accuracy rate was obtained while training the network with Inceptionv3 model.

After training the network with Inceptionv3 model, as seen in Table 9, F-measure value of 89.99%, Specificity value of 100%, Sensitivity value of 81.81%, FPR value 0, FDR value 0, FNR value 0.1818 and accuracy value of 88.06% were obtained.

As seen in the Confusion matrix given in table 9, the Inceptionv3 correctly classified 36 of 36 normal images. In addition, he predicted 23 of 31 brain tumor images correctly, and 8 predicted brain tumor images

incorrectly.

The accuracy and loss curve obtained while training the network with the Googlenet model is given in Fig. 9. As seen in Figure 9, 71.64% accuracy rate was obtained while training the network with Googlenet model.

After training the network with Googlenet model, as seen in Table 10, F-measure value of 66.03%, Specificity value of 92.85%, Sensitivity value of 66.03%, FPR value 0.0714, FDR value 0.0278, FNR value 0.3396 and accuracy value of 71.64% were obtained.

As seen in the Confusion matrix given in Table 10, the Googlenet correctly classified 35 of 36 normal images. However, he estimated 1 normal images as brain tumors. In addition, he predicted 13 of 31 brain tumor images correctly, and 18 predicted brain tumor images incorrectly.

While the accuracy curve of all models used in this study is shown in Fig. 10, the loss curve is presented on Fig. 11.

When Fig. 10 and Fig. 11 are examined, the highest accuracy and least loss are obtained in the model that developed.

FPR value, FDR value, FNR value and accuracy value are presented in Table 11.

The accuracy and loss values of the models used in this study are given in Table 12. Since the loss values are very small, the loss value of each model is multiplied by 100 to increase the appearance.

Some studies used in the classification of Brain Tumor are examined in Table 13.

Conclusion

In this paper, it is aimed to classify brain tumor images by using Cnn networks and Cnn layers. Resnet50 architecture is used as a base and a hybrid model is presented. The last 5 layers of Resnet50 architecture have been removed and 10 layers have been added in its place. The results of the hybrid model developed with the 10 layers added to the last part obtained better results than the known architecture. The accuracy rate of the developed hybrid model is 97.01%. In addition, brain tumor images are classified with Alexnet, Resnet50, InceptionV3, GoogleNet and Densenet201 models. The highest accuracy rate was observed in the hybrid model developed. With the improved Resnet50 architecture presented, a remarkable improvement has been made on the accuracy of classical Resnet architecture and other architectures. This improvement is clearly illustrated by the accuracy and loss function curves in Fig. 10 and Fig. 11. Also, when the table 5-10 values are examined carefully, this improvement can be seen numerically. In future studies, it is aimed to operate different architectures by converting them into hybrid structures.

Declaration of Competing Interest

The authors declare that they have no known competing financial interests or personal relationships that could have appeared to influence the work reported in this paper.

Appendix A. Supplementary data

Supplementary data to this article can be found online at <https://doi.org/10.1016/j.mehy.2020.109684>.

References

[1] Prabhu LAJ, Jayachandran A. Mixture model segmentation system for parasagittal meningioma brain tumor classification based on hybrid feature vector. *J Med Syst* 2018;42(12):251. <https://doi.org/10.1007/s10916-018-1094-3>.

[2] Arasi PRE, Suganthi M. A clinical support system for brain tumor classification using soft computing techniques. *J Med Syst* 2019;43(5):144. <https://doi.org/10.1007/s10916-019-1266-9>.

[3] Yildirim M, Çınar A. Classification of white blood cells by deep learning methods for diagnosing disease. *Revue d'Intelligence Artificielle* 2019;33(5):335–40. <https://doi.org/10.18280/ria.330502>.

[4] Afshar, P., Mohammadi, A., & Plataniotis, K. N. (2018, October). Brain tumor type classification via capsule networks. In 2018 25th IEEE International Conference on Image Processing (ICIP) (pp. 3129–3133). IEEE.

[5] Saxena, P., Maheshwari, A., & Maheshwari, S. (2019). Predictive modeling of brain tumor: A Deep learning approach. *arXiv preprint arXiv:1911.02265*.

[6] Shahzadi, I., Tang, T. B., Meriadeau, F., & Quyyum, A. (2018, December). CNN-LSTM: Cascaded framework for brain Tumour classification. In 2018 IEEE-EMBS Conference on Biomedical Engineering and Sciences (IECBES) (pp. 633–637). IEEE.

[7] El Abbadi NK, Kadhim NE. Brain tumor classification based on singular value decomposition. *Brain* 2016;5(8).

[8] Mohsen H, El-Dahshan ESA, El-Horbaty ESM, Salem ABM. Classification using deep learning neural networks for brain tumors. *Future Comput Inf J* 2018;3(1):68–71.

[9] Charfi S, Lahmyed R, Rangarajan L. A novel approach for brain tumor detection using neural network. *Int J Res Eng Technol* 2014;2:93–104.

[10] Vani, N., Sowmya, A., & Jayamma, N. (2017). Brain Tumor Classification using Support Vector Machine. *International Research Journal of Engineering and Technology (IRJET)*, 4.

[11] Gupta T, Gandhi TK, Gupta RK, Panigrahi BK. Classification of patients with tumor using MR FLAIR images. *Pattern Recogn Lett* 2017.

[12] Çitak-Er F, Firat Z, Kovanlikaya I, Türe U, Öztürk-İsik E. Machine-learning in grading of gliomas based on multi-parametric magnetic resonance imaging at 3T. *Comput Biol Med* 2018;99:154–60.

[13] Krizhevsky, A., Sutskever, I., & Hinton, G. E. (2012). Imagenet classification with deep convolutional neural networks. In *Advances in neural information processing systems* (pp. 1097–1105).

[14] K. He X. Zhang S. Ren J. Sun. (2016). Deep residual learning for image recognition. In *Proceedings of the IEEE conference on computer vision and pattern recognition* (pp. 770–778).

[15] G. Huang Z. Liu L. Van Der Maaten K.Q. (2017). Weinberger Densely connected convolutional networks. In *Proceedings of the IEEE conference on computer vision and pattern recognition* (pp. 4700–4708).

[16] C. Szegedy V. Liu Y. Jia P. Sermanet S. Reed D. Anguelov et al. (2015). Going deeper with convolutions. In *Proceedings of the IEEE conference on computer vision and pattern recognition* (pp. 1–9).

[17] C. Szegedy V. Vanhoucke S. Ioffe J. Shlens Z. Wojna (2016). Rethinking the inception architecture for computer vision. In *Proceedings of the IEEE conference on computer vision and pattern recognition* (pp. 2818–2826).

[18] Kaggle, <https://www.kaggle.com/datasets>.

[19] E. Cengil A. Çınar E. Özbay (2017, October). Image classification with caffe deep learning framework. In 2017 International Conference on Computer Science and Engineering (UBMK) (pp. 440–444). IEEE. DOI: 10.1109/UBMK.2017.8093433.

[20] M. Yildirim A. Çınar (2019, September). Simultaneously Realization of Image Enhancement Techniques on Real-Time Fpga. In 2019 International Artificial Intelligence and Data Processing Symposium (IDAP) (pp. 1–6). IEEE. DOI: 10.1109/IDAP.2019.8875959.

[21] Pei JY, Shan P. A micro-expression recognition algorithm for students in classroom learning based on convolutional neural network. *Traitement du Signal* 2019;36(6):557–63.

[22] Liew SS, Khalil-Hani M, Bakhteri R. Bounded activation functions for enhanced training stability of deep neural networks on visual pattern recognition problems. *Neurocomputing* 2016;216:718–34. <https://doi.org/10.1016/j.neucom.2016.08.037>.

[23] Salimans, T., & Kingma, D. P. (2016). Weight normalization: A simple reparameterization to accelerate training of deep neural networks. In *Advances in neural information processing systems* (pp. 901–909).

[24] Gao W, Zhou ZH. Dropout rademacher complexity of deep neural networks. *Sci China Inform Sci* 2016;59(7):072104 <https://doi.org/10.1007/s11432-015-5470-z>.

[25] Ciresan D, Meier U, Masci J, Schmidhuber J. Multi-column deep neural network for traffic sign classification. *Neural Networks* 2012;32:333–8. <https://doi.org/10.1016/j.neunet.2012.02.023>.

[26] Montavon G, Samek W, Müller KR. Methods for interpreting and understanding deep neural networks. *Digital Signal Process* 2018;73:1–15. <https://doi.org/10.1016/j.dsp.2017.10.011>.

[27] P. Covington J. Adams E. Sargin (2016, September). Deep neural networks for youtube recommendations. In *Proceedings of the 10th ACM conference on recommender systems* (pp. 191–198). <https://doi.org/10.1145/2959100.2959190>.

[28] Matlab, www.mathworks.com/products/matlab.html.

[29] Nixon, M., Mahmoodi, S., & Zwiggelaar, R. (Eds.). (2018). *Medical Image Understanding and Analysis: 22nd Conference, MIUA 2018, Southampton, UK, July 9–11, 2018, Proceedings (Vol. 894)*. Springer. <https://doi.org/10.1007/978-3-319-95921-4>.

[30] Toraman S, Tuncer SA, Balgetir F. Is it possible to detect cerebral dominance via EEG signals by using deep learning? *Med Hypotheses* 2019;131:109315 <https://doi.org/10.1016/j.mehy.2019.109315>.